


Research Article

Nanoscale Effect Investigation for Effective Bulk Modulus of Particulate Polymer Nanocomposites Using Micromechanical Framework

Tien-Think Le ^{1,2} and Minh Vuong Le³

¹Faculty of Mechanical Engineering and Mechatronics, PHENIKAA University, Yen Nghia, Ha Dong, Hanoi 12116, Vietnam

²PHENIKAA Research and Technology Institute (PRATI), A&A Green Phoenix Group JSC, No. 167 Hoang Ngan, Trung Hoa, Cau Giay, Hanoi 11313, Vietnam

³Faculty of Engineering, Vietnam National University of Agriculture, Gia Lam, Hanoi 100000, Vietnam

Correspondence should be addressed to Tien-Think Le; think.letien@phenikaa-uni.edu.vn

Received 20 August 2020; Revised 22 February 2021; Accepted 3 March 2021; Published 15 March 2021

Academic Editor: Maria Laura Di Lorenzo

Copyright © 2021 Tien-Think Le and Minh Vuong Le. This is an open access article distributed under the Creative Commons Attribution License, which permits unrestricted use, distribution, and reproduction in any medium, provided the original work is properly cited.

This paper investigates the nanoscale effect on the effective bulk modulus of nanoparticle-reinforced polymer. An interface-based model is introduced in this work to study the nanoscale effects on the effective properties of heterogeneous materials. That interface model is able to capture discontinuity of mechanical fields across the surface between the nanoparticle and matrix. A generalized self-consistent scheme is then employed to determine the effective bulk modulus. It has been seen from the results that, in a certain range of limits, the influence of nanoscale effects on effective properties of heterogeneous materials is significant and needs to be taken into account. In particular, when the nanoparticle radius is smaller than 10 nm, the value of effective bulk modulus significantly increases when the characteristic size of nanofillers decreases. Besides, it is seen that the harder the inclusion, the smaller the nanoscale influence effects on the overall behaviors of composite materials. Finally, parametric studies in terms of surface strength and filler's volume fractions are investigated and discussed, together with a comparison between the proposed model and other contributions in the literature.

1. Introduction

As indicated by various experimental investigations using nuclear magnetic resonance (NMR), there is a disturbed area of the polymer matrix around the nanofillers. Papon et al. [1] observed that the mobility gradient distribution of the polymer matrix is significantly altered by the presence of silica nanoparticles. Using NMR, they found an area of the matrix surrounding the nanoparticles (with a thickness ranging between 2 and 14 nm) with slower dynamics. Similarly, Harton et al. [2] found an immobilized layer of the polymer matrix in the vicinity of the nanoparticle surface when experimentally investigating poly(2-vinylpyridine) reinforced with silica nanofillers. The presence of such a disturbed zone was most likely due to the inclusions and polymer chains interactions at small scales (atomic and molecular) [1, 3–7]. In terms of modeling, the

effect of such a “third phase” on the effective properties of the material is no longer negligible [8]. Therefore, it must be taken into account and modelled, especially using micromechanical multiscale techniques [9–12].

Currently, two main approaches are employed for modeling the disturbed area of the polymer matrix surrounding nanoparticles. The first approach models the disturbed area as an interphase of finite volume with unknown mechanical properties. For example, in the work of Marcadon et al. [13], the authors have investigated the interphase elastic constants using a micromechanical framework for polyethylene reinforced with silica nanoparticles. The results were compared with Molecular Dynamics simulation assuming that the interphase was isotropic linear elastic. In another study of Kim et al. [14], parameters of Molecular Dynamics such as thickness, interfacial interaction,

and interphase structural change have been used to investigate the interphase behavior using a multiscale model. Le et al. [15–17] offered a stochastic multiscale model of the interphase properties, which exhibited random spatial fluctuations from both the experimental and simulation points of view. However, according to experimental results, the relation between the interphase thickness and the nanofiller size is still a difficulty, especially when considering the behaviors at small scales (i.e., atomic and molecular scales) [18, 19]. Moreover, it is difficult to monitor the interface's mid-plane stretch using an interphase model, especially at small scales such as atomic or molecular scales [20, 21].

In the second approach, which is based on continuum mechanics, the force transmission between the nanofillers and matrix has been investigated considering an interface (an interphase with no volume). The main goal of such model is to replace the interphase model, which means that traction or displacement jumps across the interphase are equal to those of the interface [22]. This type of interface model has been effectively applied to determine the influence of nanofiller characteristic size on the effective behaviors of heterogeneous materials. For instance, in the work of Gu and He [23], the interface properties have been investigated using Taylor's expansion through a thin interphase medium. In another work [24], Benveniste has proposed an interface model to study the behavior of a thin anisotropic interphase. Numerical methods such as Finite Elements have been also used for these interface models. For example, in the work of Yvonnet et al. [25], the authors have used Finite Element Method to implement the interface model for the jumps of mechanical fields. As mentioned above, interphase models are difficult to monitor the mid-plane stretch of the interface; therefore, this is one of the most significant advantages of the proposed interface model [20], which leads to the possibility of dealing with nanoscale effects [26].

Thus, this work investigates the nanoscale effect on the effective properties of particulate polymer nanocomposites using an interface model. Section 2 describes the microstructure, homogenization scheme, and interface model. Section 3 presents the explicit calculation for obtaining the effective properties (bulk modulus) of the heterogeneous material exhibiting nanoscale effect. Finally, we present some numerical results and discuss them.

2. Materials and Methods

2.1. Description of Heterogeneous Microstructure. As depicted in Figure 1, the thickness of interphase between the matrix and the inclusion is assumed to be zero, which converts it to an interface conveying the mechanical values between the matrix and the nanofillers.

The microstructure in question comprises three phases: the nanoparticle (denoted by the subscript p), the interface Γ (denoted by subscript s), and the matrix (denoted by subscript m), respectively. The nanoparticle has a radius of r_p , whose volume fraction is denoted by f_y . The mechanical properties of the matrix and nanoparticle are considered linear, homogeneous, and isotropic. Consequently, the elasticity tensor of the nanoparticle and matrix phases is written as

$$[C^{(i)}] = \begin{bmatrix} \kappa_i + \frac{4}{3}\mu_i & \kappa_i - \frac{2}{3}\mu_i & \kappa_i - \frac{2}{3}\mu_i & 0 & 0 & 0 \\ & \kappa_i + \frac{4}{3}\mu_i & \kappa_i - \frac{2}{3}\mu_i & 0 & 0 & 0 \\ & & \kappa_i + \frac{4}{3}\mu_i & 0 & 0 & 0 \\ & & & 2\mu_i & 0 & 0 \\ \text{Sym.} & & & & 2\mu_i & 0 \\ & & & & & 2\mu_i \end{bmatrix}, \quad (1)$$

where $i = \{p, m\}$ and κ and μ are bulk and shear modulus, respectively. The mechanical property of the interface is considered spherically transversally isotropic (as it is a spherical surface surrounding the nanoparticle, with a unit normal vector n). In spherical coordinates $\{e_r, e_\theta, e_\varphi\}$, the constitutive law for the zero-volume interface is expressed as follows [27]:

$$\begin{bmatrix} \sigma_{\theta\theta}^s \\ \sigma_{\varphi\varphi}^s \\ \sigma_{\theta\varphi}^s \end{bmatrix} = \begin{bmatrix} \kappa_s + \mu_s & \kappa_s - \mu_s & 0 \\ & \kappa_s + \mu_s & 0 \\ \text{Sym.} & & 2\mu_s \end{bmatrix} \begin{bmatrix} \varepsilon_{\theta\theta}^s \\ \varepsilon_{\varphi\varphi}^s \\ \varepsilon_{\theta\varphi}^s \end{bmatrix}, \quad (2)$$

where κ_s and μ_s denote the interface bulk and shear modulus, respectively.

2.2. Jumps of Mechanical Fields across the Interface Model.

The jumps of mechanical fields such as traction or displacement fields across the interface Γ are represented below. First, let us denote the stress discontinuity at the interface by Γ . Such a jump, denoted by σ , could be expressed as

$$\sigma n = \sigma^{(m)} n - \sigma^{(p)} n = -\text{div}_s(\sigma^{(s)}), \quad (3)$$

where n is the unit normal vector, div_s is the divergence operator, and $\sigma^{(s)}$ is the stress tensor of the interface, respectively [28]. In spherical coordinates, the discontinuity of the stress field is written:

$$\sigma_{rr} e_r + \sigma_{r\theta} e_\theta + \llbracket \sigma_{r\varphi} \rrbracket e_\varphi = -\text{div}_s(\sigma^{(s)}). \quad (4)$$

The surface divergence has the following explicit form [29]:

$$\begin{aligned} \text{div}_s(\sigma^{(s)}) = & -\frac{(\sigma_{\theta\theta}^s + \sigma_{\varphi\varphi}^s)e_r}{r} \\ & + \frac{e_\theta}{r} \left[\frac{\partial \sigma_{\theta\theta}^s}{\partial \theta} + \frac{1}{\sin \theta} \frac{\partial \sigma_{\theta\varphi}^s}{\partial \varphi} + (\sigma_{\theta\theta}^s - \sigma_{\varphi\varphi}^s) \cot \theta \right] \\ & + \frac{e_\varphi}{r} \left[\frac{\partial \sigma_{\theta\varphi}^s}{\partial \theta} + \frac{1}{\sin \theta} \frac{\partial \sigma_{\varphi\varphi}^s}{\partial \varphi} + 2\sigma_{\theta\varphi}^s \cot \theta \right]. \end{aligned} \quad (5)$$

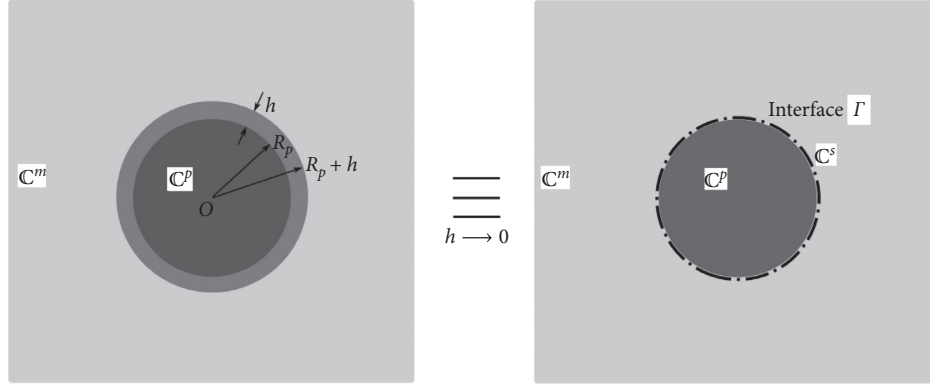


FIGURE 1: Microstructure of heterogeneous material.

Note that, in the interface model, the displacement field across Γ is continuous:

$$u = u^{(m)} - u^{(p)} = 0. \quad (6)$$

These conditions across the interface Γ will be added to the homogenization formulations to determine the effective moduli of the heterogeneous material.

2.3. Homogenization Using Generalized Self-Consistent Scheme. Homogenization technique is a two-scale method used to study the behavior of composite materials [30]. The main objective of the method is to determine the behavior of the material at the global scale based on information given from the local scale. The local scale information of the structure is numerically calculated, with the boundary conditions being mostly of the periodic type. It is worth noting that the local problem is not computed on the whole structure, but only on a representative volume element which is sufficient to represent the behavior of the whole structure. A relation between local and global scales is constructed based on the goal of minimizing the potential energy between the two scales. For more advanced developments about homogenization technique, readers are referred to the works [31–38].

In this work, the hypothesis of separation of scale was adopted [39, 40], enabling the generalized self-consistent micromechanical scheme to be used to determine the homogenized properties of the heterogeneous material [41–43]. Figure 2 depicts the homogenization scheme including the nanoparticle, the interface, the matrix phase, and the effective medium, respectively.

As the radius and volume fraction of the nanoparticle are given, the radius of the matrix phase, denoted by R_m , is deduced:

$$R_m = \left(\frac{R_p^3}{f_v} \right)^{1/3}. \quad (7)$$

The self-consistent condition for the domain V is written as

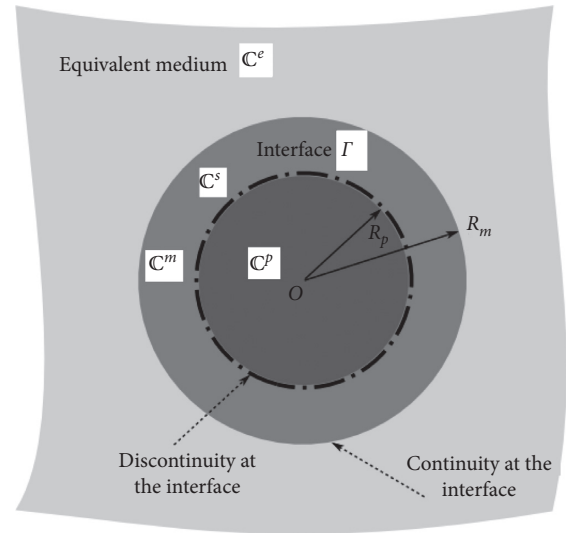


FIGURE 2: Diagram of generalized self-consistent scheme.

$$\int_{\partial V} (t u^0 - t^0 u) dS = 0, \quad (8)$$

where u and t represent the displacement and traction fields and u^0 and t^0 are the imposed displacement and stress field on the boundary of the domain, respectively. This condition was established on the basis of the self-consistency of the energy of the system.

Finally, Figure 3 presents the methodology flowchart of the present work.

3. Results and Discussion

3.1. Determination of Effective Bulk Modulus. The homogeneous isotropic strain boundary condition to determine the effective bulk modulus is represented by

$$u^0(x) = \varepsilon_0 x = \begin{pmatrix} \varepsilon_0 x \\ \varepsilon_0 y \\ \varepsilon_0 z \end{pmatrix}_{(x,y,z)}, \quad \forall x \in \partial V, \quad (9)$$

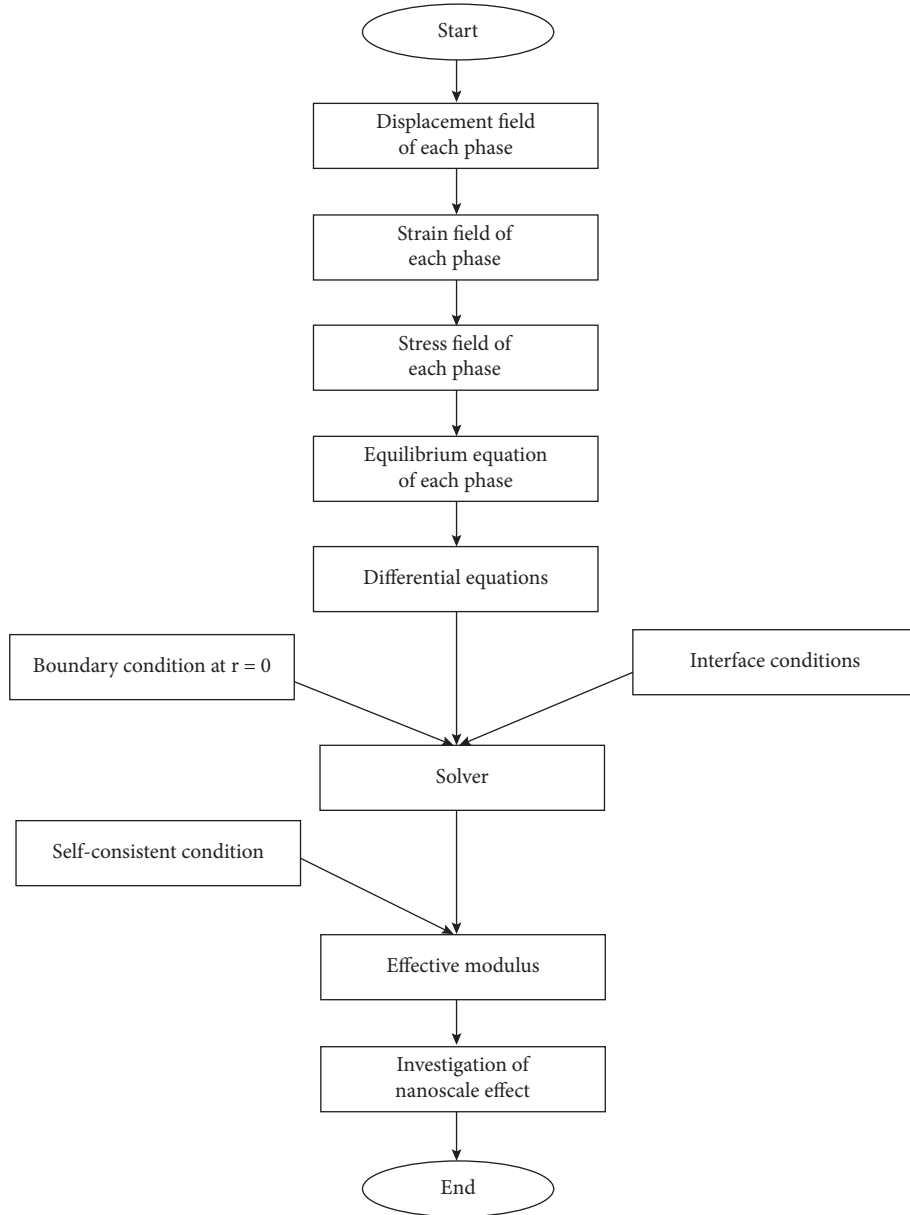


FIGURE 3: Flowchart methodology of this work.

where ε_0 is a material constant. In spherical coordinates, this condition reads

$$\begin{cases} u_r^0(x) = \varepsilon_0 r \\ u_\theta^0(x) = 0 \\ u_\varphi^0(x) = 0 \end{cases}, \quad \forall x \in \partial V. \quad (10)$$

Applying the above boundary conditions, the displacement solution can be expressed as

$$\begin{cases} u_r^{(i)} = f^{(i)}(r) \\ u_\theta^{(i)} = 0 \\ u_\varphi^{(i)} = 0 \end{cases}, \quad (11)$$

where $i = \{p; m; e\}$ (e denotes the effective medium) and $f^{(i)}$ is an unknown function to be solved. The strain field can then be expressed as the first derivative of the displacement field such as

$$\begin{cases} \varepsilon_{rr}^{(i)} = \frac{df^{(i)}(r)}{dr}, \\ \varepsilon_{\theta\theta}^{(i)} = \frac{f^{(i)}(r)}{r}, \\ \varepsilon_{\varphi\varphi}^{(i)} = \frac{f^{(i)}(r)}{r}. \end{cases} \quad (12)$$

By virtue of Hooke's law, the stress field can be written:

$$\begin{cases} \sigma_{rr}^{(i)} = \lambda_i \text{tr}(\varepsilon^{(i)}) + 2\mu_i \frac{df^{(i)}(r)}{dr}, \\ \sigma_{\theta\theta}^{(i)} = \lambda_i \text{tr}(\varepsilon^{(i)}) + 2\mu_i \frac{f^{(i)}(r)}{r}, \\ \sigma_{\varphi\varphi}^{(i)} = \lambda_i \text{tr}(\varepsilon^{(i)}) + 2\mu_i \frac{f^{(i)}(r)}{r}, \end{cases} \quad (13)$$

where λ is the Lamé elastic constant and

$$\text{tr}(\varepsilon^{(i)}) = \varepsilon_{rr}^{(i)} + \varepsilon_{\theta\theta}^{(i)} + \varepsilon_{\varphi\varphi}^{(i)} = \frac{df^{(i)}(r)}{dr} + 2\frac{f^{(i)}(r)}{r}. \quad (14)$$

In spherical coordinates, the equilibrium equation is expressed:

$$\frac{\partial \sigma_{rr}^{(i)}}{\partial r} + \frac{1}{r} (2\sigma_{rr}^{(i)} - \sigma_{\theta\theta}^{(i)} - \sigma_{\varphi\varphi}^{(i)}) = 0. \quad (15)$$

The differential equation obtained is of the form

$$r^2 \frac{d^2 f^{(i)}}{dr^2} + 2r \frac{df^{(i)}}{dr} + b_1^{(i)} f^{(i)} = 0, \quad (16)$$

where $b_1^{(i)}$ are the constants as a function of λ_i and μ_i :

$$b_1^{(i)} = \frac{-2(\lambda_i + 5\mu_i)}{\lambda_i + 2\mu_i}. \quad (17)$$

The form of the function f is such that

$$f^{(i)} = A_i r^{(3\alpha_i-1)/2} + B_i r^{-(3\alpha_i+1)/2}, \quad (18)$$

where α_i is a material parameter defined by He and Benveniste [44]. In this case with an isotropic material, α_i is equal to 1. On the other hand, A_i and B_i are unknown constants, where $i = \{p; m; e\}$. It should be pointed out that, at $r=0$, the function f must be finite. Moreover, as r tends toward infinity, the homogeneous strain boundary conditions need to be satisfied. Thus, we obtain $B_p = 0$ and $A_e = \varepsilon_0$. Such simplification allows us to reduce the number of unknown constants to 4, which are solved by applying the conditions across the interface between the nanoparticle and matrix, and those between the matrix and equivalent medium, respectively. At the interface between the nanoparticle and matrix, there is discontinuity of the stress field and continuity of the displacement field, respectively. Such conditions are written:

$$\begin{cases} u_r^{(m)} - u_r^{(p)} = 0, \\ \sigma_{rr}^{(m)} - \sigma_{rr}^{(p)} - \frac{1}{r} (\sigma_{\theta\theta}^{(s)} + \sigma_{\varphi\varphi}^{(s)}) = 0. \end{cases} \quad (19)$$

At the interface between the matrix and equivalent medium, the mechanical values are continuous across the interface. Therefore,

$$\begin{cases} u_r^{(e)} - u_r^{(m)} = 0, \\ \sigma_{rr}^{(e)} - \sigma_{rr}^{(m)} = 0. \end{cases} \quad (20)$$

A linear system of equations is then obtained that allows us to calculate A_p , A_m , B_m , and B_e , respectively. Finally, we obtain the effective bulk modulus of the heterogeneous material, as a function of the mechanical properties of different material phases and geometrical parameters:

$$\kappa_{eff} = \frac{12\kappa_m \kappa_s R_m^3 + 12\kappa_p \mu_m R_p^4 - 12\kappa_m \mu_m R_p^4 + 16\kappa_s \mu_m R_p^3 + 9\kappa_p \kappa_m R_p R_m^3 + 12\kappa_m \mu_m R_p R_m^3}{9\kappa_m R_p^4 - 9\kappa_p R_p^4 - 12\kappa_s R_p^3 + 12\kappa_s R_m^3 + 9\kappa_p R_p R_m^3 + 12\mu_m R_p R_m^3}. \quad (21)$$

3.2. Investigation of Nanoscale Effect on Effective Bulk Modulus. The nanoscale effect on the effective bulk modulus is presented in this section. Various works have set out to determine the elastic surface moduli, for instance, by using stress simulation [45], atomistic simulation [46], contrasting between the atomistic simulation and continuum model [47], semi-analytical method [48, 49], and the asymptotic approach [40, 50]. In this work, we adopted the formulation proposed by Quang and He [40] to generate the surface moduli:

$$\begin{cases} \kappa_s = \frac{hE_s}{1 - \nu_s^2}, \\ \mu_s = \frac{hE_s}{2(1 - \nu_s)}, \end{cases} \quad (22)$$

where E_s and ν_s are the surface Young's modulus and Poisson's ratio, respectively, and h presents the thickness of

the fine interphase. In this work, different values of κ_s were considered such as 1, 3, 5, and 7 N/m, respectively. In addition, different values of volume fraction f_v were investigated such as 0.2, 0.3, 0.4, and 0.5, respectively.

On the other hand, for numerical application, the elastic moduli of the matrix and nanoparticle are chosen as $E_m = 6$ GPa, $\nu_m = 0.25$; $E_p = 11.5$ GPa, $\nu_p = 0.25$.

Let us denote the effective bulk modulus with and without interface effects such as K_{eff} and κ_{eff}^0 , respectively. It is worth noting that the case without interface effects means that the change of mechanical fields such as traction or displacement between the matrix and inclusion is assumed to be continuous. In this study, we focus on investigating the ratio between κ_{eff} and κ_{eff}^0 to determine the robustness of the proposed scheme.

Figure 4 presents the results of nanoscale effect, as a function of characteristic size of nanofillers, surface modulus, and volume fraction of nanoparticle, respectively. It can be seen that the effects of characteristic size of nanofillers

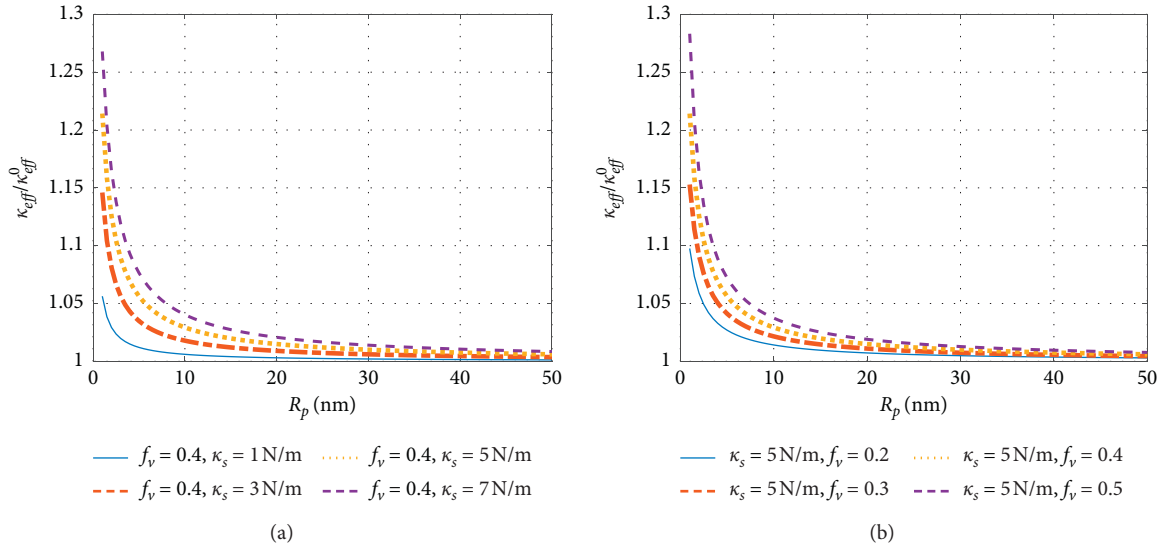


FIGURE 4: Nanoscale effect on bulk modulus as a function of (a) κ_s and (b) f_y .

are mostly detected when the nanoparticle radius is smaller than 10 nm. In particular, the effective bulk modulus increases when the nanoparticle radius decreases. On the other hand, when the characteristic size of nanofillers is greater than 30–40 nm, their effects on the effective bulk modulus are unnoticeable (i.e., $\kappa_{\text{eff}}/\kappa_{\text{eff}}^0$ ratio is smaller than 1.02, equivalent to a maximum increase of 2% in bulk modulus). This observation shows that when the characteristic size of reinforcement becomes nanometric [9, 10, 51, 52], the interface plays a significant role in the effective behavior of the material. On the other hand, in terms of the volume fraction of the nanoparticle, it did not show any significant impact on the effective bulk modulus [53, 54].

Moreover, as shown in Figure 4(a), the nanoscale effect increases with increasing interface modulus. For instance, at $R_p = 2$ nm and $f_y = 0.4$, the $\kappa_{\text{eff}}/\kappa_{\text{eff}}^0$ ratios are 1.029, 1.081, 1.126, and 1.165, when κ_s are 1, 3, 5, and 7 N/m, respectively. It should be noted that the higher the strength (energy) of the interface, the greater the effect on the effective properties. As observed in Figure 4(b), the size effects are proportional to the inclusion volume fraction, between the solutions with and without the interface. For instance, at $R_p = 2$ nm and $\kappa_s = 5$ N/m, $\kappa_{\text{eff}}/\kappa_{\text{eff}}^0$ ratios are 1.059, 1.091, 1.126, and 1.164, when f_y are 0.2, 0.3, 0.4, and 0.5, respectively. The degree of influence of the interface on the effective behaviors is also proportional to the volume fraction of the inclusions, as they are dependent on each other.

3.3. Comparison with Existing Models. In this section, we compare the results of the framework proposed in this study and other frameworks existing in the literature, as in the work of Firooz et al. [52], Zemlyanova and Mogilevskaya [55], Nazarenko et al. [56], Duan et al. [22], and Gu et al. [57]. The formulae, interface models, and homogenization techniques used to compute the effective bulk modulus for each paper are expressed in Table 1.

Material properties used to compute the effective bulk modulus of 6 models are indicated in Table 2. Figures 5(a)–5(c) show the comparison of the effective bulk modulus between the framework proposed in this paper and 5 other frameworks in the literature, with the volume fraction $f_y = 0.2, 0.4, \text{ and } 0.6$, respectively, in function of the radius of the nanoparticle R_p . The contrast of elastic properties (i.e., Young's modulus) between the nanoparticle and the matrix in this case is fixed at 10. It can be seen that good agreement between all the solutions for the bulk modulus was obtained; i.e., the model used in this work and other models in the literature have a stronger correlation. However, for the case of Duan et al. [22], a slight difference was observed for particle radius smaller than 10 nm. Moreover, for the case of $f_y = 0.2$, the model proposed by Firooz et al. [52] also exhibited a difference compared to others. It is interesting to notice that Duan et al. [22] and Firooz et al. [52] have used composite spheres assemblage and Mori-Tanaka method for the homogenization scheme. Moreover, a general interface model has been developed in Firooz et al. [52]. Besides, Table 3 summarizes the values of $\kappa_{\text{eff}}/\kappa_{\text{eff}}^0$ for each framework at $R_p = 1$ nm and $R_p = 50$ nm. We can see that when the volume fraction increases, the ratio values (especially when $R_p = 1$ nm) become close to each other.

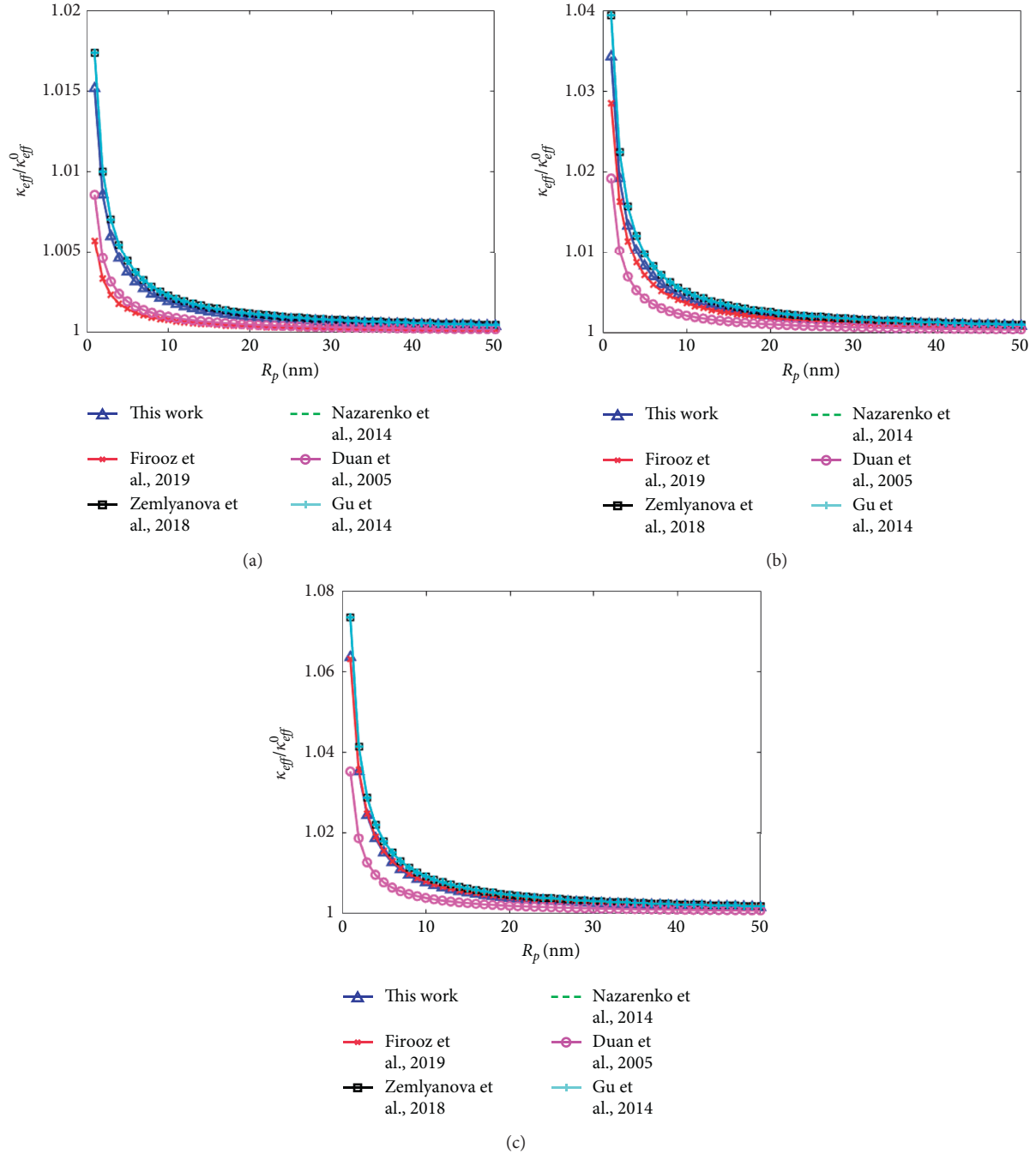
Figures 6(a)–6(d) show the comparison of the effective bulk modulus between the framework proposed in this paper and 5 other frameworks in the literature, with the contrast of elastic properties (i.e., Young's modulus) between the particle and the matrix $E_p/E_m = 10, 20, 30, \text{ and } 1000$, respectively, in function of the radius of the nanoparticle R_p . Such a comparison reveals the influence of particle to matrix stiffness ratio on the overall bulk modulus (for very stiff and very soft inclusions, respectively). The volume fraction of the inclusion used in this case is fixed at 0.4. It is seen that the higher the E_p/E_m ratio, the smaller the nanoscale effect we have on the overall behavior of the material.

TABLE 1: Formulae for prediction of effective bulk modulus of nanocomposites taking into account nanoscale effect.

Ref.	Expression	Interface model	Homogenization technique
Firooz et al. [52]	$\kappa_{eff} = 3R_p [\kappa_m (3\kappa_p + 4\mu_m) + 4f_v \mu_m (\kappa_p - \kappa_m)] + 4[\lambda_s + \mu_s] [3\kappa_m + 4f_v \mu_m] / (3R_p) [3\kappa_p + 4\mu_2 + 3f_v (\kappa_m - \kappa_p)] + 12[1 - f_v] [\lambda_s + \mu_s]$	Simplified general interface model that recovers the elastic (stress-type) interface model	Composite sphere assemblage method
Zemlyanova and Mogilevskaya [55]	$\kappa_{eff} / \kappa_m = 3\kappa_p + 4\mu_m + 2\eta_s + 4f_v \mu_m (\kappa_p / \kappa_m - 1 + 2\eta_s / (3\kappa_m)) / (3\kappa_p + 4\mu_m + 2\eta_s - 3f_v (\kappa_p - \kappa_m + 2\eta_s / 3)), \text{ where } \eta_s = 2(\lambda_s + \mu_s / R_p)$	Steigmann-Ogden interface model	Equivalent particle (particle-plus-interface) + Maxwell's homogenization approach
Nazarenko et al. [56]	$\kappa_{eff} = f_v [\kappa_p + \kappa_s] + (1 - f_v) \kappa_m + (9f_v (1 - f_v) \kappa [\kappa_p - \kappa_m + \kappa_s]^2 / (1 - 9\kappa [f_v \kappa_m + (1 - f_v) (\kappa_p + \kappa_s) - \kappa_c])$ this case are the Lamé parameters of the reference medium, which is chosen as the matrix medium	Gurtin-Murdoch interface model	Energy-equivalent inhomogeneity
Duan et al. [22]	$\kappa_{eff} = 3\kappa_p (3\kappa_m + 4f_v \mu_m) + 2\mu_m [4f_v \mu_m \kappa_s^2 + 3\kappa_m (2 - 2f_v + \kappa_s^2)] / (3[3(1 - f_v) \kappa_p + 3f_v \mu_m (2 + \kappa_s^2 - f_v \kappa_s^2)]$, where $\kappa = 1/9(\lambda_c + 2\mu_c)$	Gurtin-Murdoch interface model	Equivalent particle (particle-plus-interface) + composite spheres assemblage
Gu et al. [57]	$\kappa_{eff} = \kappa_m + (f_v (\kappa^{eq} - \kappa_m) (3\kappa_m + 4\mu_m)) / (3(1 - f_v) (\kappa^{eq} - \kappa_m) + 3\kappa_m + 4\mu_m)$, where $\kappa^{eq} = \kappa_p + (4/3)(\kappa_s / R)$	Gurtin-Murdoch interface model	Equivalent particle (particle-plus-interface) + generalized self-consistent method
This work	$\kappa_{eff} = 12\kappa_m \kappa_s R_m^3 + 12\kappa_p \mu_m R_p^4 - 12\kappa_m \mu_m R_p^4 + 16\kappa_s \mu_m R_p^4 + 9\kappa_p \kappa_m R_p^3 + 12\kappa_m \mu_m R_p^3 R_m^3 / (9\kappa_m R_p^4 - 9\kappa_p R_p^4 - 12\kappa_s R_p^3 + 12\kappa_s R_m^3 + 9\kappa_p R_p^3 + 12\mu_m R_p^3 R_m^3)$	Gurtin-Murdoch interface model	Generalized self-consistent method

TABLE 2: Material properties used to compute the effective bulk modulus of 6 models.

E_m (GPa)	ν_m	E_p (GPa)	ν_p	f_v	$\lambda_s = \mu_s$ (N/m)
6	0.25	11.5	0.25	0.4	1

FIGURE 5: Comparison of effective bulk modulus ratio curves between 6 models, in function of nanoparticle radius, with (a) $f_v = 0.2$, (b) $f_v = 0.4$, and (c) $f_v = 0.6$, and $E_p/E_m = 10$.

It is seen that the higher the E_p/E_m ratio, the smaller the nanoscale effect on the effective properties of nanocomposites. From an experimental point of view, the effects of polymer/particle interactions on polymer chain dynamics and on mechanical properties of nanocomposites have been

widely investigated, sometimes with non-conclusive evidence. The importance of interactions, like covalent bonds or hydrogen bonds, among the surface of inorganic fillers and the organic matrix has been shown at a molecular level by, for example, Avolio et al. [58] and Nicola et al. [59].

TABLE 3: Values of the $\kappa_{\text{eff}}/\kappa_{\text{eff}}^0$ ratio between different frameworks in the case where the contrast of elastic properties is fixed and the volume fraction is varied.

Ref.	$f_y = 0.2,$ $R_p = 1$	$f_y = 0.2,$ $R_p = 50$	$f_y = 0.4,$ $R_p = 1$	$f_y = 0.4,$ $R_p = 50$	$f_y = 0.6,$ $R_p = 50$	$f_y = 0.6,$ $R_p = 50$
This work	1.0151	1.0004	1.0343	1.0009	1.0636	1.0016
Firooz et al. [52]	1.0057	1.0002	1.0286	1.0008	1.0632	1.0016
Zemlyanova and Mogilevskaya [55]	1.0174	1.0005	1.0395	1.0010	1.0735	1.0019
Nazarenko et al. [56]	1.0174	1.0005	1.0395	1.0010	1.0735	1.0019
Duan et al. [22]	1.0085	1.0002	1.0193	1.0004	1.0353	1.0008
Gu et al. [57]	1.0151	1.0004	1.0343	1.0009	1.0636	1.0016

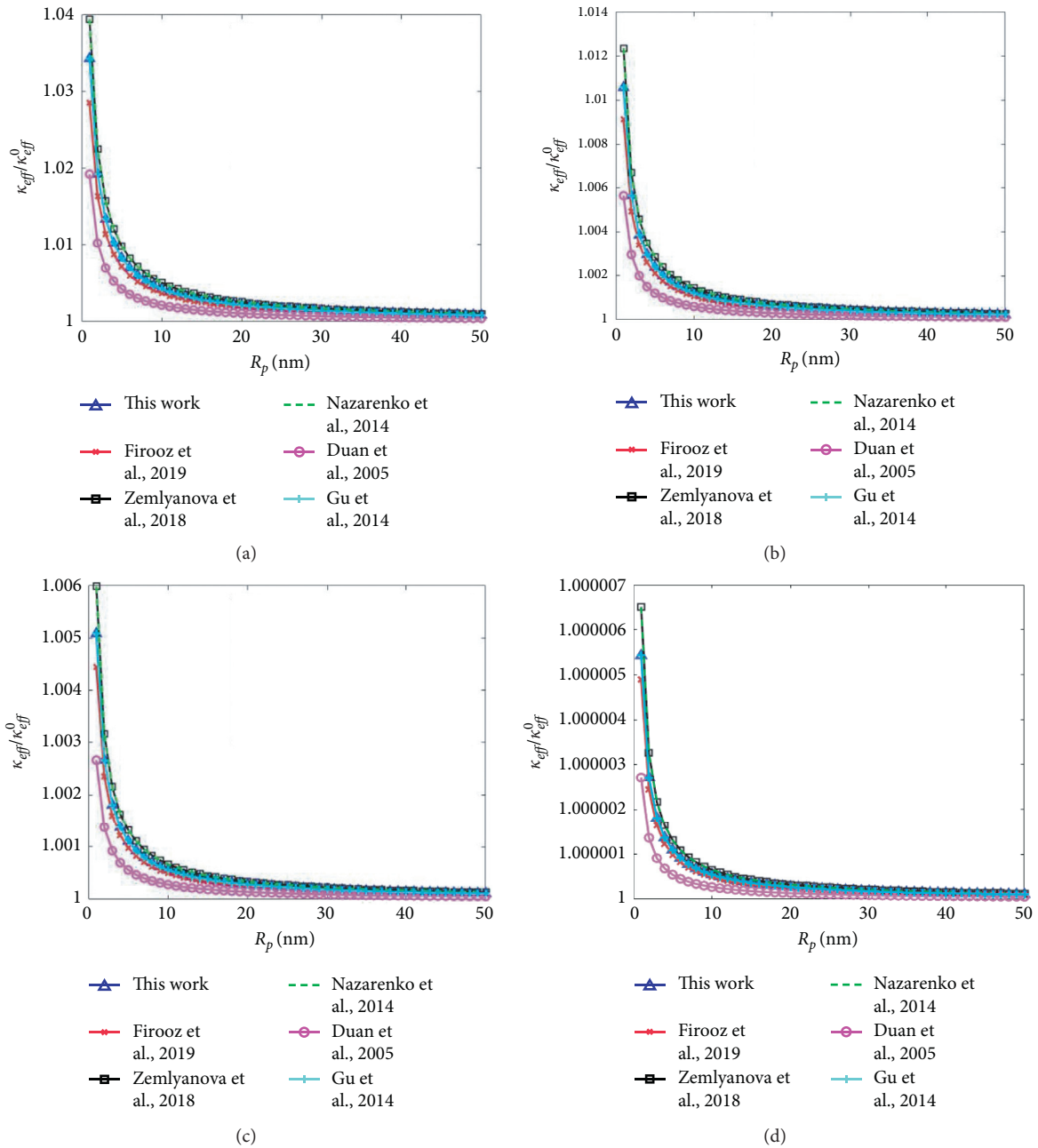


FIGURE 6: Comparison of effective bulk modulus ratio curves between 6 models, in function of nanoparticle radius, with $f_v = 0.4$ and (a) $E_p/E_m = 10$, (b) $E_p/E_m = 20$, (c) $E_p/E_m = 30$, and (d) $E_p/E_m = 10^3$.

However, the effect of such interactions on experimentally measured macroscopic properties is not easy to rationalize.

In several experimental studies, nanoscale effect on the effective properties of heterogeneous materials has been clearly shown, particularly for polymers reinforced with spherical nanofillers. For example, in the work of Douce et al. [60], the inclusion size effect on the effective behavior (tensile modulus) of nanocomposite has been investigated. Three different inclusion diameters have been used for the comparison such as 15, 35, and 60 nm. In particular, it can be noted, for example, that the effective tensile modulus was 4.3 and 3.95 GPa for the inclusions whose diameters are 15 and 35 nm, respectively. However, the effects of 60 nm particles were not observed in this case. A possible explanation is that, for this size of reinforcements (i.e., larger than 50 nm in diameter), the nanoparticles tend to form aggregates, which are responsible for the very significant increase of the modulus. Most recently, Blivi et al. [61] have explored experimental evidence of size effect in silica-reinforced poly(methyl methacrylate). Uniaxial tensile tests have been carried out and showed that Young's modulus has increased in decreasing particle size (particle sizes are 500, 150, 60, and 25 nm and volume fraction of reinforcement is kept constant). Finally, other experimental results on nanoscale effect are available, such as [61–64].

For a micromechanics modeling point of view, the proposed model can be used to retrieve information on the interface/interphase formation and properties [51, 53]. More precisely, formation of the interphase is exhibited by its thickness, whereas properties of the interphase are directly related to the thickness and the interface parameters (bulk and shear surface moduli). Thus, if the interface parameters are known, the interphase properties can be computed through an inverse identification. On the other hand, the prediction of nanocomposites overall properties accounting for interphase/interface effect is much more complex *in real systems* because of various aspects such as the following:

- (i) The thickness of interphase in function of particle distribution size, shape of nanoparticle, and temperature [13, 40, 42, 65–67]
- (ii) Existence of both nanoparticulate agglomeration phenomenon and free nanoparticles in real systems [66, 68]
- (iii) Existence of overlapping interphase in real systems [69–72]
- (iv) Stochastic analysis being required in most cases [73, 74, 75, 76, 77, 78, 79]

4. Conclusions

In this work, an interface model was integrated into the classical homogenization scheme to explore the nanoscale effect of materials reinforced with nanometric fillers. To this end, the mechanical values across the surface between the nanofiller and matrix exhibited discontinuities, which were captured by the interface model. The effective modulus of the material was then derived based on the generalized self-

consistent micromechanical scheme. It was shown that the effective bulk modulus depended on the characteristic size of fillers, especially when they are nanometric in scale. Moreover, the effective modulus depended on the surface strength and the volume fraction of the fillers.

The comparison with experimental data (mostly for measurement of Young's modulus of nanocomposites) will be considered in our next research, where effective bulk, shear, and Young's moduli are expressed as a function of surface parameters. In this work, we mainly focus on the nanoscale effect on the effective behaviour of heterogeneous materials in the elastic regime. In future works, other regimes such as elastoplastic or viscoplastic can be taken into account for this type of study. In addition, besides using numerical method such as Finite Element Method, Molecular Dynamics can also be applied to study the atomic and molecular scales. At present, there is a shortfall in such simulations coupling continuum mechanics and atomistic simulations to model the interface region between the matrix and nanofillers.

Data Availability

The data used to support the findings of this study are available from the corresponding author upon request.

Conflicts of Interest

The authors declare that there are no conflicts of interest regarding the publication of this paper.

Acknowledgments

The authors thank Prof. J. Guilleminot (Duke University, Durham, USA), for his helpful advice and comments on this paper.

References

- [1] A. Papon, K. Saalwächter, K. Schäler, L. Guy, F. Lequeux, and H. Montes, "Low-field NMR investigations of nanocomposites: polymer dynamics and network effects," *Macromolecules*, vol. 44, no. 4, pp. 913–922, 2011.
- [2] S. E. Harton, S. K. Kumar, H. Yang et al., "Immobilized polymer layers on spherical nanoparticles," *Macromolecules*, vol. 43, no. 7, pp. 3415–3421, 2010.
- [3] C. Wan and B. Chen, "Reinforcement and interphase of polymer/graphene oxide nanocomposites," *Journal of Materials Chemistry*, vol. 22, no. 8, pp. 3637–3646, 2012.
- [4] T.-T. Le, "Prediction of tensile strength of polymer carbon nanotube composites using practical machine learning method," *Journal of Composite Materials*, vol. 55, no. 6, p. 787, 2020.
- [5] T.-T. Le, *Modélisation stochastique, en mécanique des milieux continus, de l'interphase inclusion-matrice à partir de simulations en dynamique moléculaire*, PhD Thesis, University of Paris-Est Marne-la-Vallée, Paris, France, 2015.
- [6] C. Soize, "Stochastic representations and statistical inverse identification for uncertainty quantification in computational mechanics," in *Proceedings of the UNCECOMP 2015, 1st ECCOMAS Thematic International Conference On Uncertainty Quantification In Computational Sciences And*

- Engineering*, pp. 1–26, May 2015, <https://hal-upec-upem.archives-ouvertes.fr/hal-01158252>.
- [7] T.-T. Le, “Analysis of elastic deformation of amorphous polyethylene in uniaxial tensile test by using molecular dynamics simulation,” *Computer Methods in Materials Science*, vol. 20, pp. 38–44, 2020.
 - [8] S.-Y. Fu, X.-Q. Feng, B. Lauke, and Y.-W. Mai, “Effects of particle size, particle/matrix interface adhesion and particle loading on mechanical properties of particulate-polymer composites,” *Composites Part B: Engineering*, vol. 39, no. 6, pp. 933–961, 2008.
 - [9] S. Firooz and A. Javili, “Understanding the role of general interfaces in the overall behavior of composites and size effects,” *Computational Materials Science*, vol. 162, pp. 245–254, 2019.
 - [10] A. Javili, P. Steinmann, and J. Mosler, “Micro-to-macro transition accounting for general imperfect interfaces,” *Computer Methods in Applied Mechanics and Engineering*, vol. 317, pp. 274–317, 2017.
 - [11] Y. Zare, “Development of Halpin-Tsai model for polymer nanocomposites assuming interphase properties and nanofiller size,” *Polymer Testing*, vol. 51, pp. 69–73, 2016.
 - [12] D. P. Bach, D. Brancherie, and L. Cauvin, “Size effect in nanocomposites: XFEM/level set approach and interface element approach,” *Finite Elements in Analysis and Design*, vol. 165, pp. 41–51, 2019.
 - [13] V. Marcadon, D. Brown, E. Hervé, P. Mélé, N. D. Albrera, and A. Zaoui, “Confrontation between Molecular Dynamics and micromechanical approaches to investigate particle size effects on the mechanical behaviour of polymer nanocomposites,” *Computational Materials Science*, vol. 79, pp. 495–505, 2013.
 - [14] B. Kim, J. Choi, S. Yang, S. Yu, and M. Cho, “Multiscale modeling of interphase in crosslinked epoxy nanocomposites,” *Composites Part B: Engineering*, vol. 120, pp. 128–142, 2017.
 - [15] T. T. Le, J. Guilleminot, and C. Soize, “Stochastic continuum modeling of random interphases from atomistic simulations. Application to a polymer nanocomposite,” *Computer Methods in Applied Mechanics and Engineering*, vol. 303, pp. 430–449, 2016.
 - [16] T.-T. Le, “Probabilistic modeling of surface effects in nano-reinforced materials,” *Computational Materials Science*, vol. 186, Article ID 109987, 2021.
 - [17] T.-T. Le, “Probabilistic investigation of the effect of stochastic imperfect interfaces in nanocomposites,” *Mechanics of Materials*, vol. 151, Article ID 103608, 2020.
 - [18] J. Choi, H. Shin, S. Yang, and M. Cho, “The influence of nanoparticle size on the mechanical properties of polymer nanocomposites and the associated interphase region: a multiscale approach,” *Composite Structures*, vol. 119, pp. 365–376, 2015.
 - [19] I. Chung and M. Cho, “Recent studies on the multiscale Analysis of polymer nanocomposites,” *Multiscale Science and Engineering*, vol. 1, no. 3, pp. 167–195, 2019.
 - [20] A. Esmaeili, P. Steinmann, and A. Javili, “Non-coherent energetic interfaces accounting for degradation,” *Computational Mechanics*, vol. 59, no. 3, pp. 361–383, 2017.
 - [21] T.-T. Le, “Multiscale Analysis of elastic properties of nano-reinforced materials exhibiting surface effects. Application for determination of effective shear modulus,” *Journal of Composites Science*, vol. 4, no. 4, p. 172, 2020.
 - [22] H. L. Duan, J. Wang, Z. P. Huang, and B. L. Karihaloo, “Size-dependent effective elastic constants of solids containing nano-inhomogeneities with interface stress,” *Journal of the Mechanics and Physics of Solids*, vol. 53, no. 7, pp. 1574–1596, 2005.
 - [23] S. T. Gu and Q. C. He, “Interfacial discontinuity relations for coupled multifield phenomena and their application to the modeling of thin interphases as imperfect interfaces,” *Journal of the Mechanics and Physics of Solids*, vol. 59, no. 7, pp. 1413–1426, 2011.
 - [24] Y. Benveniste, “A general interface model for a three-dimensional curved thin anisotropic interphase between two anisotropic media,” *Journal of the Mechanics and Physics of Solids*, vol. 54, no. 4, pp. 708–734, 2006.
 - [25] J. Yvonnet, H. L. Quang, and Q.-C. He, “An XFEM/level set approach to modelling surface/interface effects and to computing the size-dependent effective properties of nanocomposites,” *Computational Mechanics*, vol. 42, no. 1, pp. 119–131, 2008.
 - [26] H. Le Quang, T.-L. Phan, and G. Bonnet, “Effective thermal conductivity of periodic composites with highly conducting imperfect interfaces,” *International Journal of Thermal Sciences*, vol. 50, no. 8, pp. 1428–1444, 2011.
 - [27] H. L. Duan, J. Wang, Z. P. Huang, and Z. Y. Luo, “Stress concentration tensors of inhomogeneities with interface effects,” *Mechanics of Materials*, vol. 37, no. 7, pp. 723–736, 2005.
 - [28] M. E. Gurtin and A. Ian Murdoch, “A continuum theory of elastic material surfaces,” *Archive for Rational Mechanics and Analysis*, vol. 57, no. 4, pp. 291–323, 1975.
 - [29] H. L. Duan, J. Wang, Z. P. Huang, and B. L. Karihaloo, “Eshelby formalism for nano-inhomogeneities,” *Proceedings of the Royal Society A: Mathematical, Physical and Engineering Sciences*, vol. 461, no. 2062, pp. 3335–3353, 2005.
 - [30] E. Sanchez-Palencia, “Homogenization method for the study of composite media,” *Asymptotic Analysis II*, vol. 985, pp. 192–214, 1983.
 - [31] G. Allaire, *Shape Optimization by the Homogenization Method*, Springer Science & Business Media, Berlin, Germany, 2012.
 - [32] N. S. Bakhvalov and G. Panasenko, *Homogenisation: Averaging Processes in Periodic Media: Mathematical Problems in the Mechanics of Composite Materials*, Springer Science & Business Media, Berlin, Germany, 2012.
 - [33] A. Bensoussan and J. L. Lions, *Asymptotic Analysis for Periodic Structures*, American Mathematical Society, Providence, RI, USA, 2011.
 - [34] D. Cioranescu and P. Donato, *An Introduction to Homogenization*, Oxford University Press, Oxford, UK, 1999.
 - [35] G. Dal Maso, *An Introduction to Γ -Convergence*, Springer Science & Business Media, Berlin, Germany, 2012.
 - [36] G. W. Milton and A. T. Sawicki, “Theory of composites. Cambridge monographs on applied and computational mathematics,” *Applied Mechanics Reviews*, vol. 56, 2003.
 - [37] M. V. Le, J. Yvonnet, N. Feld, and F. Detrez, “FULL-FIELD elastic simulations for image-based heterogeneous structures with a coarse mesh condensation multiscale method,” *International Journal for Multiscale Computational Engineering*, vol. 18, no. 3, p. 305, 2020.
 - [38] M. V. Le, J. Yvonnet, N. Feld, and F. Detrez, “The Coarse Mesh Condensation Multiscale Method for parallel computation of heterogeneous linear structures without scale separation,” *Computer Methods in Applied Mechanics and Engineering*, vol. 363, Article ID 112877, 2020.
 - [39] H. L. Duan, X. Yi, Z. P. Huang, and J. Wang, “A unified scheme for prediction of effective moduli of multiphase

- composites with interface effects. Part I: theoretical framework,” *Mechanics of Materials*, vol. 39, no. 1, pp. 81–93, 2007.
- [40] H. L. Quang and Q.-C. He, “Variational principles and bounds for elastic inhomogeneous materials with coherent imperfect interfaces,” *Mechanics of Materials*, vol. 40, no. 10, pp. 865–884, 2008.
- [41] R. M. Christensen and K. H. Lo, “Solutions for effective shear properties in three phase sphere and cylinder models,” *Journal of the Mechanics and Physics of Solids*, vol. 27, no. 4, pp. 315–330, 1979.
- [42] H. L. Quang and Q.-C. He, “Size-dependent effective thermoelastic properties of nanocomposites with spherically anisotropic phases,” *Journal of the Mechanics and Physics of Solids*, vol. 55, no. 9, pp. 1899–1931, 2007.
- [43] N. X. Ho and T.-T. Le, “Effects of variability in experimental database on machine-learning-based prediction of ultimate load of circular concrete-filled steel tubes,” *Measurement*, vol. 176, Article ID 109198, 2021.
- [44] Q. He and Y. Benveniste, “Exactly solvable spherically anisotropic thermoelastic microstructures,” *Journal of the Mechanics and Physics of Solids*, vol. 52, no. 11, pp. 2661–2682, 2004.
- [45] P. Müller and A. Saúl, “Elastic effects on surface physics,” *Surface Science Reports*, vol. 54, no. 5–8, pp. 157–258, 2004.
- [46] V. B. Shenoy, “Atomistic calculations of elastic properties of metallic fcc crystal surfaces,” *Physical Review B*, vol. 71, no. 9, Article ID 094104, 2005.
- [47] C. Sievers, J. Mosler, L. Brendel, and P. Kurzeja, “Computational homogenization of material surfaces: from atomistic simulations to continuum models,” *Computational Materials Science*, vol. 175, Article ID 109431, 2020.
- [48] R. Dingreville and J. Qu, “A semi-analytical method to estimate interface elastic properties,” *Computational Materials Science*, vol. 46, no. 1, pp. 83–91, 2009.
- [49] R. Dingreville and J. Qu, “A semi-analytical method to compute surface elastic properties,” *Acta Materialia*, vol. 55, no. 1, pp. 141–147, 2007.
- [50] J. Wang, H. L. Duan, Z. Zhang, and Z. P. Huang, “An anti-interpenetration model and connections between interphase and interface models in particle-reinforced composites,” *International Journal of Mechanical Sciences*, vol. 47, no. 4-5, pp. 701–718, 2005.
- [51] Y. Zhu and J. Woody Ju, “Interface energy effect on effective elastic moduli of spheroidal particle-reinforced nanocomposites,” *Acta Mechanica*, vol. 231, no. 7, pp. 2697–2709, 2020.
- [52] S. Firooz, G. Chatzigeorgiou, F. Meraghni, and A. Javili, “Homogenization accounting for size effects in particulate composites due to general interfaces,” *Mechanics of Materials*, vol. 139, Article ID 103204, 2019.
- [53] Y. Koutsawa, S. Tiem, W. Yu, F. Addiego, and G. Giunta, “A micromechanics approach for effective elastic properties of nano-composites with energetic surfaces/interfaces,” *Composite Structures*, vol. 159, pp. 278–287, 2017.
- [54] W. Xu, F. Wu, Y. Jiao, and M. Liu, “A general micro-mechanical framework of effective moduli for the design of nonspherical nano- and micro-particle reinforced composites with interface properties,” *Materials & Design*, vol. 127, pp. 162–172, 2017.
- [55] A. Y. Zemlyanova and S. G. Mogilevskaya, “On spherical inhomogeneity with steigmann-ogden interface,” *Journal of Applied Mechanics*, vol. 85, no. 12, Article ID 121009, 2018.
- [56] L. Nazarenko, S. Bargmann, and H. Stolarski, “Closed-form formulas for the effective properties of random particulate nanocomposites with complete Gurtin-Murdoch model of material surfaces,” *Continuum Mechanics and Thermodynamics*, vol. 29, no. 1, pp. 77–96, 2017.
- [57] S.-T. Gu, J.-T. Liu, and Q.-C. He, “Size-dependent effective elastic moduli of particulate composites with interfacial displacement and traction discontinuities,” *International Journal of Solids and Structures*, vol. 51, no. 13, pp. 2283–2296, 2014.
- [58] R. Avolio, G. Gentile, M. Avella, D. Capitani, and M. E. Errico, “Synthesis and characterization of poly (methylmethacrylate)/ silica nanocomposites: study of the interphase by solid-state NMR and structure/properties relationships,” *Journal of Polymer Science Part A: Polymer Chemistry*, vol. 48, no. 23, pp. 5618–5629, 2010.
- [59] A. D. Nicola, “Rational design of nanoparticle/monomer interfaces: a combined computational and experimental study of in situ polymerization of silica based nanocomposites,” *RSC Advances*, vol. 5, no. 87, pp. 71336–71340, 2015.
- [60] J. Douce, J.-P. Boilot, J. Biteau, L. Scodellaro, and A. Jimenez, “Effect of filler size and surface condition of nano-sized silica particles in polysiloxane coatings,” *Thin Solid Films*, vol. 466, no. 1-2, pp. 114–122, 2004.
- [61] A. S. Blivi, F. Benhui, J. Bai, D. Kondo, and F. Bédoui, “Experimental evidence of size effect in nano-reinforced polymers: case of silica reinforced PMMA,” *Polymer Testing*, vol. 56, pp. 337–343, 2016.
- [62] E. Chabert, *Propriétés mécaniques de nanocomposites à matrice polymère: approche expérimentale et modélisation*, These de doctorat, Lyon, France, 2002.
- [63] A. Vassiliou, D. Bikiaris, K. Chrissafis, K. M. Paraskevopoulos, S. Y. Stavrev, and A. Docoslis, “Nanocomposites of isotactic polypropylene with carbon nanoparticles exhibiting enhanced stiffness, thermal stability and gas barrier properties,” *Composites Science and Technology*, vol. 68, no. 3-4, pp. 933–943, 2008.
- [64] Y. Q. Liu, H. T. Cong, W. Wang, C. H. Sun, and H. M. Cheng, “AlN nanoparticle-reinforced nanocrystalline Al matrix composites: fabrication and mechanical properties,” *Materials Science and Engineering: A*, vol. 505, no. 1-2, pp. 151–156, 2009.
- [65] A. Pontefisso, M. Zappalorto, and M. Quaresimin, “Influence of interphase and filler distribution on the elastic properties of nanoparticle filled polymers,” *Mechanics Research Communications*, vol. 52, pp. 92–94, 2013.
- [66] K. Baek, H. Shin, T. Yoo, and M. Cho, “Two-step multiscale homogenization for mechanical behaviour of polymeric nanocomposites with nanoparticulate agglomerations,” *Composites Science and Technology*, vol. 179, pp. 97–105, 2019.
- [67] D. Sokołowski and M. Kamiński, “Homogenization of carbon/polymer composites with anisotropic distribution of particles and stochastic interface defects,” *Acta Mechanica*, vol. 229, no. 9, pp. 3727–3765, 2018.
- [68] K. W. Putz, M. J. Palmeri, R. B. Cohn, R. Andrews, and L. C. Brinson, “Effect of cross-link density on interphase creation in polymer nanocomposites,” *Macromolecules*, vol. 41, no. 18, pp. 6752–6756, 2008.
- [69] S. Ma, I. Scheider, and S. Bargmann, “Ultrastrong nanocomposites with interphases: nonlocal deformation and damage behavior,” *European Journal of Mechanics-A/Solids*, vol. 75, pp. 93–108, 2019.
- [70] J. Wang and J. Luo, “Micromechanical study on the effective elastic moduli of polymer-bonded explosives with imperfect interfaces,” *Journal of Energetic Materials*, vol. 36, no. 3, pp. 278–290, 2018.

- [71] R. D. Peng, H. W. Zhou, H. W. Wang, and L. Mishnaevsky, "Modeling of nano-reinforced polymer composites: micro-structure effect on Young's modulus," *Computational Materials Science*, vol. 60, pp. 19–31, 2012.
- [72] S.-L. Gao and E. Mäder, "Characterisation of interphase nanoscale property variations in glass fibre reinforced polypropylene and epoxy resin composites," *Composites Part A: Applied Science and Manufacturing*, vol. 33, no. 4, pp. 559–576, 2002.
- [73] H. C. Phan, T. T. Le, N. D. Bui, H. T. Duong, and T. D. Pham, "An empirical model for bending capacity of defected pipe combined with axial load," *International Journal of Pressure Vessels and Piping*, vol. 192, p. 104368, 2021.
- [74] J. Guilleminot, T. T. Le, and C. Soize, "Stochastic framework for modeling the linear apparent behavior of complex materials: application to random porous materials with inter-phases," *Acta Mechanica Sinica*, vol. 29, no. 6, pp. 773–782, 2013.
- [75] T.-T. Le, "Practical machine learning-based prediction model for axial capacity of square CFST columns," *Mechanics of Advanced Materials and Structures*, pp. 1–16, 2020, in press.
- [76] T.-T. Le, "Practical hybrid machine learning approach for estimation of ultimate load of elliptical concrete-filled steel tubular columns under axial loading," *Advances in Civil Engineering*, vol. 2020, Article ID e8832522, 19 pages, 2020.
- [77] K. A. Acton and S. C. Baxter, "Characterization of random composite properties based on statistical volume element partitioning," *Journal of Engineering Mechanics*, vol. 144, no. 2, Article ID 4017168, 2018.
- [78] T.-T. Le and M. V. Le, "Development of user-friendly kernel-based Gaussian process regression model for prediction of load-bearing capacity of square concrete-filled steel tubular members," *Materials and Structures*, vol. 54, no. 2, 2021.
- [79] B. Staber and J. Guilleminot, "Stochastic modeling and generation of random fields of elasticity tensors: a unified information-theoretic approach," *Comptes Rendus Mécanique*, vol. 345, no. 6, pp. 399–416, 2017.